



This is the accepted manuscript made available via CHORUS. The article has been published as:

Critical slowing down in sudden quench dynamics

Ceren B. Dağ, Yidan Wang, Philipp Uhrich, Xuesen Na, and Jad C. Halimeh

Phys. Rev. B **107**, L121113 — Published 28 March 2023

DOI: [10.1103/PhysRevB.107.L121113](https://doi.org/10.1103/PhysRevB.107.L121113)

Critical slowing down in sudden quench dynamics

Ceren B. Dağ,^{1,2,*} Yidan Wang,^{2,†} Philipp Uhrich,³ Xuesen Na,⁴ and Jad C. Halimeh³

¹*ITAMP, Harvard-Smithsonian Center for Astrophysics, Cambridge, Massachusetts, 02138, USA*

²*Department of Physics, Harvard University, 17 Oxford Street Cambridge, MA 02138, USA*

³*INO-CNR BEC Center and Department of Physics,*

University of Trento, Via Sommarive 14, I-38123 Trento, Italy

⁴*Simons Laufer Mathematical Sciences Institute, 17 Gauss Way, Berkeley, CA 94720, USA.*

We reveal a prethermal dynamical regime upon suddenly quenching to the vicinity of a quantum phase transition in the time evolution of 1D spin chains. The prethermal regime is analytically found to be self-similar, and its duration is governed by the ground-state energy gap. Based on analytical insights and numerical evidence, we show that this dynamical regime universally exists independently of the location of the probe site, the presence of weak interactions, or the initial state. The resulting prethermal dynamics leads to an out-of-equilibrium scaling function of the order parameter in the vicinity of the transition. **Our theory suggests that sudden quench dynamics, besides probing quantum phase transitions, may give rise to a universal critical slowing down near the critical point.**

Out-of-equilibrium quantum many-body physics has recently been at the forefront of theoretical and experimental investigations in condensed matter physics [1] due to recent impressive progress in the control and precision achieved in quantum synthetic matter [2–11]. Not only have concepts from equilibrium physics been extended to the out-of-equilibrium realm such as with dynamical phase transitions [12–16] and dynamical scaling laws [14, 17–22], but there have also been concerted efforts to probe equilibrium quantum critical points (QCPs) and universal scaling laws through quench dynamics [17, 19, 21, 23–29] or with infinite-temperature initial states [30–32]. Such techniques obviate the need for undertaking the usually difficult task of cooling the system into its ground state over a range of its microscopic parameters in order to construct its equilibrium phase diagram. The underlying concept behind these works is of the Landau paradigm [12], i.e., it is based on non-analytic behavior in the long-time dynamics of a local order parameter. This indicates that, in principle, such nonanalytic behavior may be used to extract equilibrium criticality that manifests itself dynamically.

It is well known that relaxation times of order parameters (OP) diverge at QCP after adiabatic quenches [9, 33, 34]. Such divergent behavior of the order parameter is a signature of the nonanalyticity at the QCP and is often referred as *critical slowing down*. While the current focus of the literature is to utilize sudden quenches in probing the QCP, how the relaxation time of the order parameter behaves around the QCP after a sudden quench has not been sufficiently explored [19, 21, 33, 35–37]. In fact, intriguingly, it has been found that some 1D short-range models relax the fastest at the QCP [21, 33, 35, 36], contrary to the common intuition of critical slowing down. Dynamical order parameters for these models also do not exhibit nonanalyticity at the QCP [21, 36, 38].

In this Letter, we introduce boundaries to short-range

1D spin systems and probe single-site OPs. This reveals a universal prethermal regime upon suddenly quenching to the vicinity of a QCP, when a nonanalyticity of the dynamical order parameter is present at the QCP. Phrased differently, we show the presence of critical slowing down of order parameter dynamics near a QCP after a sudden quench. **Intuitively**, we find that the duration of the prethermal regime is determined by the inverse energy gap. The universality of the regime holds true for different probe sites, initial conditions, and weak integrability breaking. Further, we analytically and numerically show that this *critically prethermal* regime gives rise to a non-linear scaling function for the dynamical order parameter in the reduced control parameter of the QCP. We present our discussion based on a paradigmatic model of QCPs, the transverse-field Ising chain (TFIC).

Our work provides new insights on probing quantum criticality in sudden quench dynamics: Quantum criticality does not only affect the stationary regime, but its signature is also visible in a new dynamical regime emerging before the stationary regime. Therefore, sudden quench dynamics does not only probe quantum phase transitions as has been found so far by many [23–27, 29, 40], but also gives rise to a universal and critical slowing down near QCP.

Dynamical regimes of TFIC.— The short-range TFIC with interaction strength Δ is given by

$$H = -J \sum_{r=1}^{N-1} \sigma_r^z \sigma_{r+1}^z - \Delta \sum_{r=1}^{N-2} \sigma_r^z \sigma_{r+2}^z + h \sum_{r=1}^N \sigma_r^x, \quad (1)$$

where $\sigma_r^{x,z}$ are the Pauli spin matrices on sites r , h is the transverse-field strength, N is the length of the chain, and we fix $J = 1$, which sets the energy scale of the system. In equilibrium, the TFIC has two phases, i) the ferromagnetically ordered phase for $h < h_c$ and ii) the paramagnetic disordered phase for $h \geq h_c$, where h_c is the QCP. At $\Delta = 0$, this model becomes the nearest-neighbor (n.n.) TFIC with a QCP $h_c = 1$, and the

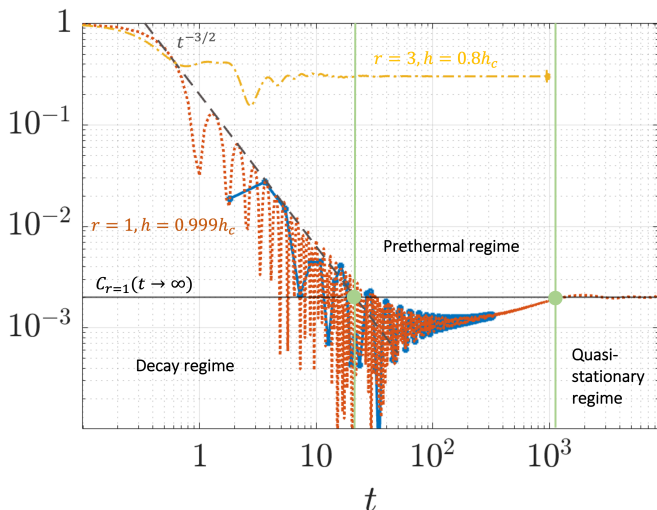


Figure 1. The edge magnetization $C_{r=1}(t)$ for the Hamiltonian Eq. (1) with $\Delta = 0$ after a quench in the transverse-field strength from $h_i = 0$ to the vicinity of the QCP at h_c . The red-dotted curve is plotted based on Eq. (3) for a semi-infinite chain [39]. The blue-squares are values of $|C_1(t, h)|$ obtained numerically for the open-boundary TFIC with a system size of $N = 1440$, the method of which is detailed in Ref. [40]. The panels show the three regimes of time evolution separated by green vertical lines: the decay regime with a power-law decay $\sim t^{-3/2}$ (dashed-gray line) on the left, the prethermal regime in the middle and the quasi-stationary (q.s.) regime on the right. The horizontal black line is $1 - h^2$, the q.s. value for $r = 1$. The onsets of prethermal and q.s. regimes are marked with green balls. As a comparison, the yellow dotted-dashed line plots $|C_{r=3}(t, h)|$ away from the QCP at $h = 0.8h_c$ for $N = 1500$ spins and a quench from $h_i = 0$ where there is no prethermal regime.

model is integrable. The QCP shifts to favor order upon introducing interactions with $\Delta > 0$. The order parameter for this QCP is the magnetization averaged over all sites; when it is finite, it indicates spontaneous symmetry breaking in the ground state and the system is in the ordered phase.

We consider as initial state the ground state $|\psi_0\rangle$ of H at initial value h_i of the transverse-field strength, and then we quench the latter to a value h . In a periodic chain, the single-site magnetization $C_r(t) = \langle \psi_0 | \sigma_r^z(t) | \psi_0 \rangle$, at any site r , decays exponentially to zero for any h [21, 38, 41, 42], and hence $C_r(t \rightarrow \infty)$ does not host nonanalyticity at the QCP [21, 38]. On the other hand, in an open-boundary chain, $C_r(t)$ stabilizes to a finite nonzero value when $t \rightarrow \infty$ at any r within a finite distance to the boundary, so long as $h_i < h < h_c$. This dynamical regime is called quasi-stationary (q.s.) regime [40, 43]; see Fig. 1. For $h \geq h_c$, $C_r(t \rightarrow \infty) = 0$ is suggested by numerical results [40, 43] and some analytical arguments [40]. In our joint paper [40], a kink observed at the QCP becomes sharper as the system size increases, and this suggests a nonanalyticity

in $C_r(t \rightarrow \infty)$. The origin of this nonanalyticity depends on the presence of zero modes which are induced in the open-boundary chain [40]. In particular, for the edge magnetization ($r = 1$) with $\Delta = 0$ and $h_i = 0$, there exists a simple analytic form in the infinite time limit $C_1(t \rightarrow \infty) = 1 - h^2 \equiv C_1^{qs}$ for $h < 1$ and $C_1(t \rightarrow \infty) = 0$ for $h \geq 1$ [40, 43, 44].

The single-site magnetization at any r away from the QCP approaches the q.s. regime as $t^{-3/2}$ after an exponential decay so long as $h_i < h$ [43]. Upon quenching to the vicinity of the QCP the decay trend is described only by the power law $t^{-3/2}$. Additionally, an intermediate dynamical regime emerges preceding the q.s. regime (see Fig. 1)—the nonequilibrium response dips below the q.s. value and eventually ramps up to it. Figure 1 shows the time evolution of the edge magnetization $C_1(t)$ when the system is quenched from $h_i = 0$, e.g., $|\psi_0\rangle = |\uparrow \dots \uparrow\rangle$ to $h = 0.999$, in the integrable (n.n.) TFIC both numerically and analytically [39], where we observe this intermediate regime marked as *prethermal regime*. The onsets t_{pt} and t_{qs} of the prethermal and q.s. regimes, respectively, are where the decay roughly ends, i.e. $t_{pt}^{-3/2} \sim C_1^{qs}$, and where a stationary value is attained in the time evolution, respectively (vertical lines in Fig. 1). To probe and characterize this prethermal regime, we first define a reduced control parameter $h_n \equiv (h_c - h)/h_c$ as the distance to the QCP and $\delta C_r(t, h_n) \equiv C_r[t, h = h_c(1 - h_n)] - C_r(t, h = h_c)$, which we name *critical response*. As $h_n \rightarrow 0$, $C_1^{qs}(h_n) \approx 2h_n$, we arrive at $t_{pt} \propto h_n^{-2/3}$. The punchline of our paper is that when $h_n \rightarrow 0$ and $t \gg 1$, the critical response for general r takes the universal form

$$\delta C_r(t, h_n) = C_r^{qs}(|h_n|) f_{\Delta, h_i}(h_n t), \quad (2)$$

where $f_{\Delta, h_i}(h_n t)$ depends on the weak interaction strength Δ and the initial condition h_i . Note that $C_r^{qs}(|h_n|)$ is the q.s. value in the ordered phase, while Eq. (2) works on both sides of the QCP. Further, $f_{\Delta, h_i}(h_n t)$ is a continuous function of $h_n t$ that satisfies $f_{\Delta, h_i}(h_n t = 0) = 1/2$ and $f_{\Delta, h_i}(h_n t) = 1 - f_{\Delta, h_i}(-h_n t)$. When $|h_n|t \gg 1$, $f_{\Delta, h_i}(h_n t)$ approaches 1 in the ordered phase ($h_n > 0$) and approaches 0 in the disordered phase ($h_n < 0$), demonstrating the nonanalyticity in the q.s. value across the QCP. We plot $f_{\Delta, h_i}(h_n t)$ for $h_i = 0$ and $h_n t > 0$ in Figs. 2(a) and 2(b), for $\Delta = 0$ and $\Delta = 0.1$ [45], respectively.

Eq. (2) suggests that the onset of the the q.s. regime scales with h_n as $t_{qs} \propto h_n^{-1}$, hence the duration of the prethermal regime follows $\Delta t \equiv t_{qs} - t_{pt} \propto h_n^{-1}$. As the energy of the zero-momentum state in the integrable TFIC is $\epsilon_{k=0} = h_n$ [46], the prethermal duration $\Delta t \propto \epsilon_{k=0}^{-1}$ is inversely proportional to the single-particle energy gap. The prethermal regime lasts longer as we approach the QCP, motivating the name *critically prethermal regime* and justifying $\delta C_r(t, h_n)$ as the critical response.

In the following, we analytically derive $f_{\Delta, h_i}(h_n t)$ for the edge magnetization at $\Delta = 0$ and $h_i = 0$, and numerically demonstrate that it holds true for different probe sites r .

Prethermal regime in the integrable TFIC.— The edge magnetization has an analytic series expression whose derivation can be found in [40],

$$C_1(t, h) = \sum_{m=0}^{\infty} \frac{(-1)^m}{(2m)!} (2t)^{2m} N_m(h^2), \quad (3)$$

$$N_m(h^2) = \sum_{n=1}^m N_{mn} h^{2n}, \quad N_{mn} = \frac{1}{m} \binom{m}{n-1} \binom{m}{n},$$

where $N_m(x)$ are the Narayana polynomials [47, 48]. Eq. (3) also describes the two-time edge correlators in the Kitaev chain at infinite temperature [30]. It has an analytical expression $C_1(t, h = 1) = J_1(4t)/(2t)$ at the QCP [40] where $J_1(t)$ is the Bessel function of the first kind. Additionally, we note that Eq. (3) is a generating function of Narayana polynomials and can be expressed in terms of inverse Laplace transform of a closed form function [49]. This alternative expression is useful in probing the critically prethermal regime and deriving $f_{\Delta, h_i}(h_n t)$. The critical response in the vicinity of the QCP $h_n \rightarrow 0$ follows [49]

$$\delta C_1(t, h_n) = C_1^{qs}(|h_n|) \left[-\frac{1}{2} J_0(4t) + f(h_n t) \right] + O(h_n^2), \quad (4a)$$

$$f(h_n t) \equiv \frac{1}{2} - \sum_{n=1}^{\infty} \frac{(-h_n t)^{2n-1}}{(2n)!} \chi_n, \quad (4b)$$

where $\chi_n \equiv (-1)^{1-n} 2^{1-2n} (2n-2)! / (n-1)!^2$. $\delta C_1(t, h_n)/C_1^{qs}(h_n)$ for $h_n = 0.005$ based on Eq. (4a) is plotted as a black-solid line in Fig. 2(a). Here the term $-\frac{1}{2} C_1^{qs}(|h_n|) J_0(4t)$, where $J_0(t)$ is the Bessel function of the first kind, introduces oscillations that become negligible when $t \gg 1$. This term also originates from a high frequency expansion in the derivation [49], which is why it is only an early-time effect, and hence nonuniversal. The function $f(h_n t)$ can be written in terms of a generalized Hypergeometric function $f(h_n t) = \frac{1}{2} + \frac{(h_n t)}{2} {}_1F_2 \left[\left\{ \frac{1}{2} \right\}; \left\{ \frac{3}{2}, 2 \right\}; -(h_n t)^2 \right]$ [49], and it is plotted in Fig. 2(a) with a dotted-red line. In contrast to the nonuniversal term, $f(h_n t)$ originates from a low frequency—long-wavelength—expansion in the derivation, and hence providing extra evidence that the prethermal regime is critical. **Let us note in passing that the rescaling of time with h_n that emerges from the microscopic calculation is consistent with the Ising universality class ($\nu = z = 1$) [46].**

Next we demonstrate Eq. (2) in the ordered phase using numerics for a finite-size system ($N = 1440$). Because our numerics is based on the cluster theorem in the space-time limit [38], we obtain numerical values of $|C_r(t, h_n)|$,

and hence use $\delta|C_r|(t, h_n) \equiv ||C_r(t, h_n)| - |C_r(t, 0)||$ to approximate $\delta C_r(t, h_n)$ [40, 50]. Our numerical data shows that, for $h_n \rightarrow 0$, and $t \gg 1$, $\delta C_r(t, h)$ for different choices of r are proportional to each other. Hence defining $\eta_r = C_1^{qs}(h_n) \delta|C_r|(t', h_n) / \delta|C_1|(t', h_n)$, we found numerically that η_r does not depend on t' as long as $t' \gg 1$ [51]. For the edge spin, $\eta_1 = C_1^{qs}(h_n)$ by definition. Refs. [43, 52] show that the q.s. values of the bulk spins have an exponentially decaying spatial profile in r , suggesting $\eta_r \approx C_1^{qs}(h_n) e^{-(r-1)/\xi(h_n)}$, where $\xi(h_n)$ is the correlation length [49]. **Then the q.s. regime value at any r tends to zero linearly in h_n as $h_n \rightarrow 0$.**

Fig. 2(a) plots $\delta|C_r|(t \geq 50, h_n)/\eta_r$ for all $r = 1, 3, 6, 9, 12$ quenched from an initial state $h_i = 0$ to $h_n \in [9 \times 10^{-4}, 0.05]$. The colors, from dark blue to light cyan, correspond to decreasing h_n , respectively. The time axis is rescaled by the distance to the QCP, h_n . For Fig. 2(a), $t' = 280$ is chosen in η_r . The data collapses on top of each other, and matches well with the analytical function $f(h_n t)$ for $h_n t \gg 0.1$. Therefore, we have numerically demonstrated the validity of Eq. (2) for different probe sites $r > 1$ in the ordered phase, and hence $f_{0,0}(h_n t) = f(h_n t)$.

Discussion for $\Delta, h_i \neq 0$.— In this section, we discuss Eq. (2) and $f_{\Delta, h_i}(h_n t)$ for general Δ and h_i . We present the case of $\Delta = 0.1$ as an example of the near-integrable model which can be treated with quench mean-field theory (qmFT) [40, 45]. In this case, the QCP is shifted to $h_c \approx 1.165$, and numerical evidence shows that the location of the nonanalyticity observed in the dynamical order parameter is no longer equal to the QCP [40]. Hence in [40], we define a dynamical critical point (DCP) based on the nonanalyticity following Ref. [27], and find it to be $h_{dc} = 1.1437$. Since qmFT maps the interacting problem back to a noninteracting problem, we also apply single-particle energy gap analysis in [40], and show that the gap for this noninteracting model indeed closes at $h_{dc} = 1.1437$. Therefore, it is natural to anticipate that a possible critically prethermal regime should emerge around h_{dc} for $\Delta \neq 0$, motivating a definition of the reduced control parameter as $h_n = (h_{dc} - h)/h_{dc}$.

Fig. 2(b) verifies Eq. (2) for $\Delta = 0.1$ in the ordered phase using qmFT numerics for $r = 1, 3, 6, 9, 12$ quenched from an initial state $h_i = 0$ to $h_n \in [8.74 \times 10^{-4}, 0.0557]$. Our joint work [40] shows that for small Δ , $C_1^{qs}(h) = \alpha(h_{dc}^\nu - h^\nu)$ where α and ν are numerically extracted as $\alpha = 0.81$ and $\nu = 1.81$ for $\Delta = 0.1$. Note that for $\alpha = 1, \nu = 2$ and $h_{dc} = h_c = 1$, we recover the q.s. value of the edge spin in the integrable TFIC $C_1^{qs}(h) = 1 - h^2$. Hence, $C_1^{qs}(h_n) = \alpha h_{dc}^\nu [1 - (1 - h_n)^\nu]$, and we use this expression to define η_1 . η_r for $r \neq 1$ are defined similarly as in the integrable case. Importantly, we find that all data for $\delta|C_r|(t \geq 50, h_n)/\eta_r$ collapse on top of each other, which confirms the validity of Eq. (2) for small $\Delta \neq 0$. However, the data does not match with the function $f_{0,0}(h_n t)$ (red-dotted line in Fig. 2(b)), suggest-

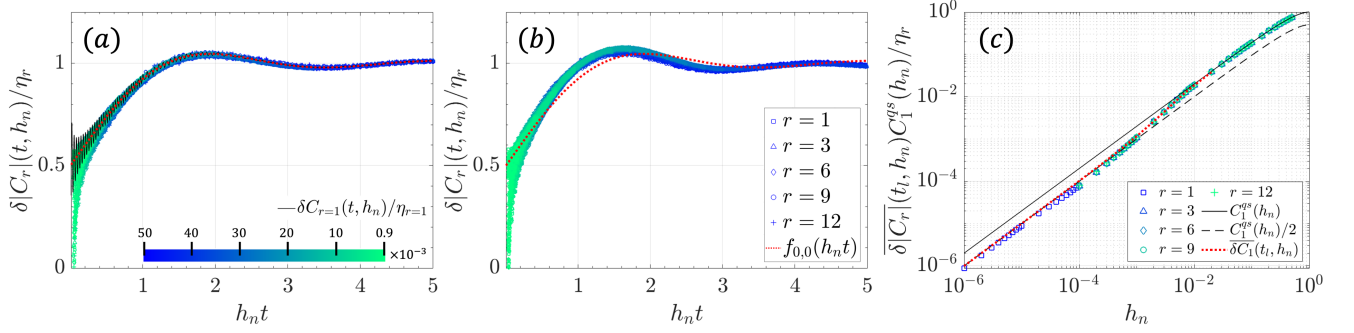


Figure 2. Numerical rescaled critical response $\delta|C_r|(t, h_n)/\eta_r$ for (a) $\Delta = 0$, the integrable TFIC and (b) $\Delta = 0.1$, a near-integrable TFIC quenched from $h_i = 0$ to $h_n \in [9 \times 10^{-4}, 0.05]$ (colorbar). The system size is $N = 1440$ and the numerical data is for probe sites $r = 1, 3, 6, 9, 12$. The rescaling factor $\eta_r = C_1^{qs}(h_n)\delta|C_r|(t', h)/\delta|C_1|(t', h)$ is independent of the choice of t' and can be understood as the numerical evaluation of the q.s. value $C_r^{qs}(h_n)$. For the plots, $t' = 280$. As a comparison, the analytical value of $\delta C_1(t, h_n)/C_1^{qs}(h_n)$ is plotted in (a) (black-solid) and $r = 1$ $f_{0,0}(h_n t) = f(h_n t)$ in Eq. (4b) (red-dotted) is plotted in both (a) and (b). (c) The dynamical OP for the integrable TFIC with cutoffs $t^* = 20$ and $t_l = 330$. The numerical data for different r collapse on top of $\delta C_1(t_l, h_n)$, Eq. (6) (red-dotted). When t_l is in the decay ($t_l h_n \gg 1$) or q.s. ($t_l h_n \ll 1$) regimes, the data is described by $C_1^{qs}(h_n)/2$ (dashed-black line) and $C_1^{qs}(h_n)$ (solid-black line), respectively, both linear in h_n when $h_n \ll 1$. When t_l is in the prethermal regime ($h_n t_l \sim 1$), the data deviates from the linear functions in the two ends.

ing that $f_{\Delta, h_i}(h_n t)$ depends on Δ . In the SM, we verify Eq. (2) numerically for $h_i \neq 0$ and show that $f_{\Delta, h_i}(h_n t)$ also depends on h_i .

For all Δ , h_i and r considered, $C_r^{qs}(|h_n|) \sim |h_n|$ as $h_n \rightarrow 0$. Specifically, when $\Delta = 0$, $C_r^{qs}(|h_n|) = 2^{2-r}|h_n| + O(|h_n|^{3/2})$ for $\Delta = 0$, and $C_1^{qs}(h_n) \approx \alpha \nu h_{dc}' h_n$ for $\Delta = 0.1$. The case of $h_i \neq 0$ is discussed in Ref. [40]. The linear scaling of $C_r^{qs}(|h_n|)$ in h_n results in the self-similarity of the critical response: When $h_n \rightarrow 0$, $t \gg 1$ and $\kappa t \gg 1$, $\delta C_r(t, h_n) = \kappa \delta C_r(\kappa^{-1} t, \kappa h_n)$ where κ is a rescaling factor.

Scaling of dynamical OP near QCP.— Finally, we probe the critically slowed down prethermal regime in the ordered phase ($h_n > 0$) by studying the scaling of a dynamical OP defined with a finite long-time cutoff t_l :

$$\overline{\delta C_r}(t_l, h_n) \equiv \frac{1}{t_l - t^*} \int_{t^*}^{t_l} dt \delta C_r(t, h_n), \quad (5)$$

where t^* is a short-time cutoff with negligible influence on the value of $\overline{\delta C_r}(t_l, h_n)$ [49]. This newly introduced dynamical OP extends beyond the current paradigm of probing the dynamical scaling near a QCP at infinite time, and enables the discussion of experiments often limited by finite coherence times. Here we can imagine t_l as an experimentally (or computationally) the longest time accessible. The temporal cutoff can be extended to $t_l \rightarrow \infty$ if desired.

When $t^* = 0$, Eq. (4b) together with Eq. (2) suggest that the dynamical OP for $\Delta = 0$ and $h_i = 0$ is given by

[53]

$$\overline{\delta C_r}(t_l, h_n) = C_r^{qs}(|h_n|) \left[\frac{1}{2} - \sum_{n=1}^{\infty} \frac{(-h_n t_l)^{2n-1}}{2n \times (2n)!} \chi_n \right] + O(h_n t_l^{-1}) + O(h_n^2). \quad (6)$$

$\overline{\delta C_r}(t_l, h_n)$ for $r = 1$ is plotted in Fig. 2(c) as the red-dotted line for $t_l = 330$. When $t_l \gg 1$ and $h_n \rightarrow 0$, the first line of Eq. (6) gives a good approximation of $\overline{\delta C_r}(t_l, h_n)$. For $h_n t_l \ll 1$ and $h_n t_l \gg 1$, t_l probes the beginning of the prethermal ramp and the q.s. regime, respectively. In these regimes, we observe $\overline{\delta C_1}(t_l, h_n) \approx \frac{1}{2} C_1^{qs}(h_n)$ (dashed-black) and $\overline{\delta C_1}(t_l, h_n) \approx C_1^{qs}(h_n) = 1 - (1 - h_n)^2$ (solid-black), respectively. Both are linear in h_n for $h_n \ll 1$, and connected through a nonlinear crossover when $h_n t_l \sim 1$ holds, and hence when t_l probes the prethermal ramp.

Similar to the previous discussion, we numerically define $\overline{\delta|C_r|}(t_l, h_n)$ as the time average of $\delta|C_r|(t, h_n)$ between t^* and t_l . To demonstrate that the dynamical OP has a similar scaling behavior for different r , we rescale the data using η_r and plot $\overline{\delta|C_r|}(t_l, h_n) C_1^{qs}(h_n)/\eta_r$ in Fig. 2(c). Note that $\overline{\delta|C_r|}(t_l, h_n) C_1^{qs}(h_n)/\eta_r = \overline{\delta|C_r|}(t_l, h_n)$ for $r = 1$ by definition. The linear-to-linear crossover in $\overline{\delta C_r}(t_l, h_n)$ for small $h_n > 0$, demonstrated in Fig. 2(c), is universal for any Δ and h_i , and robust against changing t_l [49], while the shape of the nonlinear crossover depends on $f_{\Delta, h_i}(h_n t)$. This is suggested by Eq. (2), where $f_{\Delta, h_i}(h_n t)$ has universal limiting properties and $C_r^{qs}(h_n)$ always has linear scaling in h_n . To demonstrate the universality, we plot the numerical data of $\overline{\delta|C_r|}(t_l, h_n) C_1^{qs}(h_n)/\eta_r$ for $\Delta = 0.1, h_i = 0$ and $\Delta = 0, h_i = 0.1$ in the SM.

Conclusion and outlook. — We discover critical slowing down in the open-boundary TFIC upon suddenly quenching to the vicinity of the QCP. This critical slowing down is expressed in Eq. (2) universally for any probe site, weak interactions or the initial state, and rigorously proven for a special case. Analytical analysis leads us to reveal self-similarity in the dynamics and find that the duration of the prethermal regime diverges as one approaches to the QCP because of the gap closing. **The critically prethermal regime in the near-integrable TFIC is also evident in time-dependent density-matrix renormalization group calculations [54]. Therefore our conclusions for weakly interacting TFIC are valid beyond the qMFT method. An interesting question to answer in the future is whether Eq. (2) is applicable in strongly interacting TFIC.**

Emerging dynamical universality in suddenly quenched TFIC suggests the presence of critical slowing down in other open-boundary short-range spin chains, e.g., XXZ chain [36]. Critical slowing down should also be manifested in other system observables that host a late-time non-analyticity in their sudden quench dynamics [27]. **How generic the critical slowing down in sudden quench dynamics beyond the Ising universality is an exciting future prospect.**

We thank Susanne Yelin for helpful discussions. C.B.D. is supported by the ITAMP grant at Harvard University. Y.W. is supported by AFOSR. J.C.H. and P.U. acknowledge support by Provincia Autonoma di Trento and the ERC Starting Grant StrEnQTh (project ID 804305), Q@TN — Quantum Science and Technology in Trento — and the Collaborative Research Centre ISOQUANT (project ID 273811115).

* ceren.dag@cfa.harvard.edu; C.D. and Y.W. contributed equally to this work.

† C.D. and Y.W. contributed equally to this work.

- [1] J. Eisert, M. Friesdorf, and C. Gogolin, *Nature Physics* **11**, 124–130 (2015).
- [2] M. Greiner, O. Mandel, T. Esslinger, T. W. Hänsch, and I. Bloch, *Nature* **415**, 39 (2002).
- [3] W. S. Bakr, J. I. Gillen, A. Peng, S. Fölling, and M. Greiner, *Nature (London)* **462**, 74 (2009).
- [4] M. Cheneau, P. Barmettler, D. Poletti, M. Endres, P. Schauß, T. Fukuhara, C. Gross, I. Bloch, C. Kollath, and S. Kuhr, *Nature* **481**, 484–487 (2012).
- [5] R. Islam, R. Ma, P. M. Preiss, M. E. Tai, A. Lukin, M. Rispoli, and M. Greiner, *Nature* **528**, 77 (2015).
- [6] A. M. Kaufman, M. E. Tai, A. Lukin, M. Rispoli, R. Schittko, P. M. Preiss, and M. Greiner, *Science* **353**, 794–800 (2016).
- [7] J. Zhang, G. Pagano, P. W. Hess, A. Kyprianidis, P. Becker, H. Kaplan, A. V. Gorshkov, Z.-X. Gong, and C. Monroe, *Nature* **551**, 601–604 (2017).
- [8] M. Gärttner, J. G. Bohnet, A. Safavi-Naini, M. L. Wall, J. J. Bollinger, and A. M. Rey, *Nature Physics* **13**, 781–786 (2017).
- [9] A. Keesling, A. Omran, H. Levine, H. Bernien, H. Pichler, S. Choi, R. Samajdar, S. Schwartz, P. Silvi, S. Sachdev, et al., *Nature* **568**, 207 (2019).
- [10] P. Scholl, M. Schuler, H. J. Williams, A. A. Eberharter, D. Barredo, K.-N. Schymik, V. Lienhard, L.-P. Henry, T. C. Lang, T. Lahaye, et al., *Nature* **595**, 233 (2021).
- [11] S. Ebadi, T. T. Wang, H. Levine, A. Keesling, G. Semeghini, A. Omran, D. Bluvstein, R. Samajdar, H. Pichler, W. W. Ho, et al., *Nature* **595**, 227 (2021).
- [12] T. Mori, T. N. Ikeda, E. Kaminishi, and M. Ueda, *Journal of Physics B: Atomic, Molecular and Optical Physics* **51**, 112001 (2018).
- [13] M. Heyl, A. Polkovnikov, and S. Kehrein, *Phys. Rev. Lett.* **110**, 135704 (2013).
- [14] N. Tsuji, M. Eckstein, and P. Werner, *Phys. Rev. Lett.* **110**, 136404 (2013).
- [15] P. Jurcevic, H. Shen, P. Hauke, C. Maier, T. Brydges, C. Hempel, B. P. Lanyon, M. Heyl, R. Blatt, and C. F. Roos, *Phys. Rev. Lett.* **119**, 080501 (2017).
- [16] N. Fläschner, D. Vogel, M. Tarnowski, B. S. Rem, D.-S. Lühmann, M. Heyl, J. C. Budich, L. Mathey, K. Senstock, and C. Weitenberg, *Nature Physics* **14**, 265 (2018).
- [17] B. Sciolla and G. Biroli, *Phys. Rev. B* **88**, 201110 (2013).
- [18] E. Nicklas, M. Karl, M. Höfer, A. Johnson, W. Muesel, H. Strobel, J. Tomkovič, T. Gasenzer, and M. K. Oberthaler, *Phys. Rev. Lett.* **115**, 245301 (2015).
- [19] A. Chiochetta, M. Tavora, A. Gambassi, and A. Mitra, *Phys. Rev. B* **91**, 220302 (2015).
- [20] V. Gurarie, *Phys. Rev. A* **100**, 031601 (2019).
- [21] C. B. Dağ and K. Sun, *Phys. Rev. B* **103**, 214402 (2021).
- [22] D. Trapin, J. C. Halimeh, and M. Heyl, (2020), [arXiv:2005.06481 \[cond-mat.stat-mech\]](https://arxiv.org/abs/2005.06481).
- [23] C. Kollath, A. M. Läuchli, and E. Altman, *Phys. Rev. Lett.* **98**, 180601 (2007).
- [24] M. Karl, H. Cakir, J. C. Halimeh, M. K. Oberthaler, M. Kastner, and T. Gasenzer, *Phys. Rev. E* **96**, 022110 (2017).
- [25] M. Heyl, F. Pollmann, and B. Dóra, *Phys. Rev. Lett.* **121**, 016801 (2018).
- [26] H.-X. Yang, T. Tian, Y.-B. Yang, L.-Y. Qiu, H.-Y. Liang, A.-J. Chu, C. B. Dağ, Y. Xu, Y. Liu, and L.-M. Duan, *Phys. Rev. A* **100**, 013622 (2019).
- [27] P. Titum, J. T. Iosue, J. R. Garrison, A. V. Gorshkov, and Z.-X. Gong, *Phys. Rev. Lett.* **123**, 115701 (2019).
- [28] P. Urich, N. Defenu, R. Jafari, and J. C. Halimeh, *Phys. Rev. B* **101**, 245148 (2020).
- [29] A. Haldar, K. Mallayya, M. Heyl, F. Pollmann, M. Rigol, and A. Das, *Phys. Rev. X* **11**, 031062 (2021).
- [30] F. J. Gómez-Ruiz, J. J. Mendoza-Arenas, F. J. Rodríguez, C. Tejedor, and L. Quiroga, *Phys. Rev. B* **97**, 235134 (2018).
- [31] C. B. Dağ, L.-M. Duan, and K. Sun, *Phys. Rev. B* **101**, 104415 (2020).
- [32] Z.-H. Sun, J.-Q. Cai, Q.-C. Tang, Y. Hu, and H. Fan, *Annalen der Physik* **532**, 1900270 (2020).
- [33] J. Dziarmaga, *Advances in Physics* **59**, 1063 (2010).
- [34] A. Polkovnikov, K. Sengupta, A. Silva, and M. Vengalattore, *Rev. Mod. Phys.* **83**, 863 (2011).
- [35] M. Eckstein, M. Kollar, and P. Werner, *Phys. Rev. Lett.* **103**, 056403 (2009).
- [36] P. Barmettler, M. Punk, V. Gritsev, E. Demler, and E. Altman, *Phys. Rev. Lett.* **102**, 130603 (2009).
- [37] M. Eckstein, M. Kollar, and P. Werner, *Phys. Rev. B*

- 81**, 115131 (2010).
- [38] P. Calabrese, F. H. L. Essler, and M. Fagotti, *Journal of Statistical Mechanics: Theory and Experiment* **2012**, P07016 (2012).
- [39] $\delta C_1(t, h_n)/C_1^{qs}(h_n)$ in Fig. 1 can be plotted using either an alternative expression for Eq. (3) or the inverse Laplace transform expression detailed in [49], as evaluating the series summation in Eq. (3) for long times becomes virtually impossible.
- [40] C. B. Dağ, P. Uhrich, Y. Wang, I. P. McCulloch, and J. C. Halimeh, (2021), [arXiv:2110.02995](https://arxiv.org/abs/2110.02995) [[cond-mat.quant-gas](https://arxiv.org/abs/2110.02995)].
- [41] P. Calabrese and J. Cardy, *Phys. Rev. Lett.* **96**, 136801 (2006).
- [42] P. Calabrese, F. H. L. Essler, and M. Fagotti, *Phys. Rev. Lett.* **106**, 227203 (2011).
- [43] F. Iglói and H. Rieger, *Phys. Rev. Lett.* **106**, 035701 (2011).
- [44] F. Iglói, G. Roósz, and Y.-C. Lin, *New Journal of Physics* **15**, 023036 (2013).
- [45] The near-integrable model is mapped to the single-particle picture and the dynamics are calculated via quench mean-field theory (qMFT). qMFT introduces next n.n. coupling and pairing to the usual Kitaev chain and simply renormalizes the n.n. coupling and pairing strengths J as well as the chemical potential h . Hence, the QCP shifts favoring order. For details of this method and the results, see [40].
- [46] S. Sachdev, [Quantum Phase Transitions](https://doi.org/10.1017/9780521876223) (Cambridge University Press, 2001).
- [47] V. P. Kostov, A. Martinez-Finkelshtein, and B. Z. Shapiro, *J. Approx. Theory* **161**, 464 (2009).
- [48] T. Mansour and Y. Sun, *Discrete Math.* **309**, 4079 (2009).
- [49] See Supplementary Material.
- [50] This is a good approximation when $C_r(t, h_n)$ and $C_r(t, 0)$ are both positive, hence it is expected to work well only in the ordered phase. This approximation is also the reason why we observe a mismatch between numerics and analytics in Fig. 2(a) for the values $h_n t \ll 1$.
- [51] This indicates that when $t' \geq t_{qs}$, $\eta_r = \delta C_r(t = \infty, h_n) = C_r^{qs}(h_n)$ can be used to numerically extract the q.s. value of spin r from finite-time data [using the fact that $C_r(t = \infty, h = 1) = 0$].
- [52] K. Sengupta, S. Powell, and S. Sachdev, *Phys. Rev. A* **69**, 053616 (2004).
- [53] Eq. (6) can also be expressed as a Hypergeometric function [49].
- [54] See Figures 22(b) and 23(b) in our joint paper [40].
- [55] T. Petersen, [Eulerian Numbers](https://doi.org/10.1007/978-1-4939-9826-5), Birkhäuser Advanced Texts Basler Lehrbücher (Springer New York, 2015).
- [56] R. Graham, D. Knuth, and O. Patashnik, [Concrete Mathematics: A Foundation for Computer Science](https://doi.org/10.1002/9781119176868), A @foundation for computer science (Addison-Wesley, 1994).